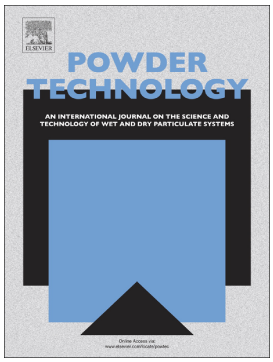

Towards a one parameter equation for a silo discharging model with inclined outlets

Marcela C. Villagrán Olivares, Jesica G. Benito, Rodolfo O. Uñac, Ana M. Vidales

PII: S0032-5910(18)30450-9
DOI: doi:10.1016/j.powtec.2018.06.010
Reference: PTEC 13443

To appear in: *Powder Technology*

Received date: 5 December 2017
Revised date: 20 February 2018
Accepted date: 4 June 2018

Please cite this article as: Marcela C. Villagrán Olivares, Jesica G. Benito, Rodolfo O. Uñac, Ana M. Vidales , Towards a one parameter equation for a silo discharging model with inclined outlets. Ptec (2017), doi:10.1016/j.powtec.2018.06.010

Towards a one parameter equation for a silo discharging model with inclined outlets

*Marcela C. Villagrán Olivares, Jesica G. Benito, Rodolfo O. Uñac, Ana M. Vidales**

INFAP, CONICET, Departamento de Física, Facultad de Ciencias Físico Matemáticas y Naturales, Universidad Nacional de San Luis, Ejército de los Andes 950, D5700HHW, San Luis, Argentina

* corresponding author, avidales@unsl.edu.ar

Abstract

Experiments on the discharge of a silo with an inclined outlet are performed for three types of seeds. The angle of inclination is varied to cover the complete range from 0º to 90º. The theoretical description of the flow rate behavior as a function of the aperture angle is achieved taking into account the two types of regimes present in the problem: *funnel* and *mass* flow. The former is assumed to be dominated by arch formation-destruction and, consequently, a free falling down of the particles from the arch dome is able to predict the experimental behavior through the addition of just one parameter closely related to the geometry of the arch. The second regime is described through a radial velocity picture for the flow streams close to the silo aperture and a numerical integration allows calculating the expected flow with good results. Finally, with the hypothesis that radial velocity can always be used as a good approximation for flow streams, an equation valid for all the range of angles is derived with the inclusion of just one parameter related to the drag force exerted by the flow on the particles. The challenge of one parameter equation for describing the mass flow rate in a wedged hopper is achieved and discussed.

Keywords: silo discharge; mass flow; funnel flow; hopper angle

1. Introduction

Silo discharge is one of the most frequent studied problems in granular matter. Two main reasons could be cited to explain this interest: the intense use of silo structures for grain manipulation in production stages and the beautiful and intriguing way in which the flow of grains develops inside them [1,2].

Since the pioneering works of Fowler and Glastonbury [3] and Beverloo et al. [4], the description of flow through apertures has progressed considerably thanks to the use of new technological tools for measurement and visualization, like fast camera videos with image processing packages, X-ray and electrical capacitance tomography and optically active materials for tracking stress chains [1,5-8]. Besides, different simulation techniques to reproduce experimental scenarios and to study the interaction of grains at the micro scale help to quantify the effect of different parameters involved in the problem, otherwise difficult to follow in a real experiment [9-12].

Concerning the theoretical description of the outflow rate, we may say that this issue is still open. The complex dynamic of the discharging process is not easy to handle analytically and the phenomenological correlation stated by Beverloo is still very robust and useful in practical problems [2, 9, 13-15].

According to the geometrical features of the silo outlet and the particles, it is well known that the flow patterns found inside a silo can be classified in two main regimes separated by one transition region. The first is the *mass flow*, where a continuous vertical descent of the material is observed throughout the silo and the hopper; this flow is expected for low friction coefficients or sufficiently inclined hopper walls. The second is the *funnel flow*, where an outflow channel is developed at the central part of the silo, above the aperture, with typical stagnant zones next to the walls; this pattern is typical for flat-bottomed hoppers. Finally, the transition regime is in between the other

two, *i.e.*, it is a combination of a funnel flow for particles next to the bottom outlet and a mass flow for particles at the top of the column. This feature is typical at low inclinations of the hopper walls [16, 17].

The main parameters involved in the development of one or the other of the above regimes are correlated by diagrams that delimit the range of values where each pattern is expected to be observed. This is very useful in silo designing, and examples of those diagrams can be found in [17-21] where the contributions of works by [22] and [23, 24] are fundamental. Nevertheless, in the diagrams correlating the hopper angle of inclination and the friction angles, the crossover between mass flow and funnel flow is not clear, sometimes it occurs sharply and other times it is represented by a more or less narrow region of uncertainty [25].

The difficulties in determining the crossover regime are in correspondence with the theoretical obstacles offered by the flow complexity. When the silo ends in a hopper with a given inclination, the Beverloo's equation is still able to describe and predict the flow rate expected only if suitable parameters are provided [2, 9, 13]. These parameters have to be determined from experiments done especially on purpose, but they are not always theoretically related to the physical variables entering the problem. Recently, good progress has been done in correlating Beverloo's parameters to the shape and size of the particles [13, 26]. Besides, old correlations exist that are of help to introduce the hopper angle dependence into the Beverloo's equation. The theoretical analysis conducted by Brown and Richards [27] arrived, under certain assumptions, to an expression for the mass flow rate where a multiplicative term depending on the angle of the hopper is introduced through minimum energy considerations. In the same line, Carleton [28] derived an expression for the flow of particles through a conical section using a force balance at the outlet of the hopper. By assuming that the dependence on

the angle of the hopper could be approximated for small angles, he arrives to a simple equation for expressing the dependence of the flow on the hopper angle.

On the other hand, Rose and Tanaka [29] proposed an empirical method to account for the hopper angle effects on the mass flow rate. Some drawbacks are associated with the use of these correlations, especially related to the difficulty of measuring some of the parameters involved in their formulation as, for instance, the angle of approach, which gives the inclination of the boundary between moving and static grains at the hopper [9, 27].

Throughout all the investigations carried out so far, it is clear that the free fall of the particles at the proximity of the outlet of the silo is the starting point to understand the flow rates found in a discharging process, at least for the case of funnel flow. Several assumptions has been made to develop theoretical or empirical correlations based on the concept that the free fall initiates at a zone just below the arches of particles that form and collapse during the discharge [4, 25, 27, 30].

To simplify the analysis, the first considerations for the shape of the arches point to a spherical dome [27, 30]. Most recently, Oldal *et al.* proposed a model based on the idea of a free fall from a parabolic shaped arch [25]. They arrived to an equation that predicts a similar behavior like Beverloo's for the funnel flow region but with no need of empirical constants. They related the unique constant entering their equation with physical considerations on the parabolic shape of the arch. Particles are assumed to start their free fall with zero initial downward velocity at the arch boundary, and the authors consider that this scenario is only valid for funnel flow regime. Indeed, the dynamic of formation and destruction of arches is observed in the funnel flow regime and has been successfully associated with the fluctuations of the flow rate during silo discharge [2, 13, 31, 32].

Given that the shape of an arch supporting a certain mass over it is a parabola, the existence of a parabolic dome at the outlet of the hopper is a suitable description for analyzing the dynamics of the discharge in the funnel flow range [33]. Nevertheless, for the mass flow regime, this assumption is no longer valid and other considerations are needed.

Continuum modelling has proven that the problem of silo discharge can also be approached from this point of view. For the case of a 2D silo, the work of Staron *et al.* [34] demonstrates a good qualitative agreement between the results obtained through a discrete element model and a continuum modelling using a Navier-Stokes solver, especially in the regions of rapid flows. In the same way, a recent work by Zheng *et al.* [35] is able to describe the mass discharge in conical hoppers by using an Eulerian-formulation finite element method (FEM) with an elastoplastic model. The results obtained for the mass discharge as a function of the angle of the hoppers are in good coincidence with other continuum formulations and discrete models, verifying the scaling of the outlet velocity and of the mass discharge with the silo aperture size.

In this work we present experimental results for the discharge of different seeds from a silo whose outlet inclination ranges from 0º to 90º, thus spanning all possible flow regimes. We make use of a simple geometrical design to visualize the internal dynamic angle of approach for the particles, *i.e.*, the angle separating the high velocity region of discharge from the stagnant one. Besides, a theoretical analysis of the dynamics of the grains as they fall in each flow regime, along with the already cited background, lead us to a one-parameter description of the whole range of silo discharging patterns.

2. Experimental set up and materials

As expressed in the Introduction, we aim to describe the mass discharge from a whole range of silo outlet inclinations. For that reason our experimental set up is designed as a quasi 2-D silo made with plexiglass as the one sketched in Figure 1. Two flat sheets form the front and rear walls of the container. The lateral walls are made with rectangular rods that can be arranged in different ways to span all possible inclinations and orifice sizes for the outlet. The thickness of the rods provides the desired thickness of the silo, L. In our experiments, L is fixed to 25 mm. The angle of inclination of the walls respect to the vertical direction is β and the outlet aperture is D, as indicated in the figure. For the case of the flat bottom silo configuration, two rectangular rods are horizontally placed and the separation between their ends provides the desired outlet orifice size D. Care is taken to avoid that particles interact with the ending edges of the rods. The other dimensions of the different parts are indicated in the figure.

Once the desired silo configuration is set, seeds are gently poured from the top with the help of an appropriate plexiglass chute. A plug at the bottom orifice prevents the outflow of the particles.

As indicated in Figure 1, the discharge of the silo is performed inside a container placed on an electronic balance Ohaus Scout, with accuracy 10^{-2} g. The balance is connected to a computer that records the mass discharged as a function of time. A typical mass vs. time plot is shown as an inset in Figure 1. From the slope of that plot, one can easily compute the discharge flow rate of the particles through a linear fit of the data.

The grains used in the experiments are three different seeds: millet, sesame and canary seed. To give an idea of their geometry, Figure 2 shows photographs of them taken with a binocular loupe. Fifty different grains for each seed type are taken for measuring their typical size though image analysis. The values obtained for the length and width of

them are reported in Table 1. The form factor, *FF*, shown there is the ratio between the mean projected length and the mean projected width of the seeds and is given just as an indicative of the elongation degree of the particles.

With the assumption that the seed's geometry can be represented by an ellipsoid of revolution with semi-axes given by its half length and half width, we are able to calculate the typical volume of a typical seed, V_{eq}, and from it, to calculate the equivalent diameter d_p (see Table 1) which represents the diameter of a sphere with the same volume V_{eq}. In this way, d_p is derived as:

$$d_p = \left(\frac{6V_{eq}}{\pi}\right)^{1/3} \tag{1}$$

The bulk density, ρ_b, for each type of grain is an important quantity participating in the discharging flow determination. The measurement of ρ_b is performed following standard procedures [13]. The apparent or bulk density is determined through the weighing of a container with known volume into which one type of seed grains is gently poured from a constant height. The mass of the seeds divided by the known volume gives rise to the values shown in Table 1, which are the average of 20 independent determinations performed for each type of seed.

3. Mass discharge modeling

As explained in the preceding sections, we perform silo discharges at different inclinations for the hopper walls starting from the flat-bottom case, β = 90º, to a completely free fall of the particles at β = 0º. The geometry of the outlet implies a

rectangular orifice with front and rear walls at zero inclination respect to the vertical. Depending on the value of β, we expect a change from mass flow regime to funnel flow as β becomes larger than θ_{app}, i.e., than the internal dynamic angle of approach for the particles. Figure 3 illustrates the situation.

For $\beta \geq \theta_{app}$, i.e., for funnel flow regime, we keep in mind the fact that the discharge is governed by a continuous mechanism of formation and destruction of arches. These arches are the result of the blockage of particles provoked by the stack of grains at the lateral stagnant zones resulting from the scarce or non movement of the particles near the outlet, whose inclination provides enough stability for the arch to survive, at least for a short period of time [2, 25]. The shape of those arches is assumed to be parabolic and their collapse means the initiation of the free fall of the particles until a new arch is created. As a consequence, the flow velocity of the particles at the outlet only depends on the height of the free fall.

Taking into account the particular geometry of our hopper, and following the ideas of Oldal et al. [25], we propose that each particle freely drops from an unstable arch geometry like the one sketched in Figure 4. The shape of the "arched gallery" is given by:

$$f(x,y) = h\left(1 - \left(\frac{2x}{D - d_p}\right)^2\right) \quad for\ all\ y \tag{2}$$

Here the height of the arch is represented by *h*, the width of the parabola is the width of the orifice, *D*, reduced by the typical diameter of the particles, which is the so called *empty annulus* correction due to the possibility that particles can sit around the border of the outlet, reducing the orifice, as can be seen in Figure 3. The shape of the parabola is

of course independent of *y*. The final velocity of a particle falling from a height $f(x,y)$ and arriving at the outlet is given by $v(x,y)=\sqrt{2gf(x,y)}$. Thus, the average velocity of the particles at the outlet orifice can be calculated as:

$$\bar{v}=\int_0^L dy\int_{-(D-d_p)/2}^{(D-d_p)/2}\sqrt{2gh\left(1-\left(\frac{2x}{D-d_p}\right)^2\right)}dx=\frac{\pi}{4}\sqrt{2g\delta\left(D-d_p\right)} \tag{3}$$

We note that the empty annulus correction is not necessary in the first integral because the walls are completely vertical and no particle can sit around those sides of the orifice. Given that the height of the parabola is very difficult to determine, even for our present geometry, we introduce in Eq. (3) the parameter $\delta=h/\left(D-d_p\right)$ which, as in [25], represents an arch shape coefficient that will be the only parameter involved in the whole description of the flow dynamics. Its value will depend on the type of grains used. In this way, the flow discharging from the silo becomes:

$$W=\frac{\pi}{4}\,\rho L\sqrt{2g\delta}\,\left(D-d_p\right)^{3/2} \tag{4}$$

To validate Eq. (4), we perform a series of silo discharges for different outlet apertures *D*, in a flat-bottomed configuration and for the three types of seeds. The experimental results are shown in Figure 5. The line curves are the corresponding fits using Eq. (4), where the best value obtained for delta is indicated in each case. These values change depending on the type of seed, showing a decrease with the increase of the form factor of the particle (see Table 1). This is in agreement with the values of delta found by Oldal *et al.* where a slight trend of decreasing is observed for the case of elongated particles [25]. This means that the more elongated the particles, the smaller is their

ability to form vaulted arches compared with the other two seeds, which seems reasonably and being in agreement with recent findings of other authors, as discussed below [36].

Eq. (4) is expected to be valid inside the funnel flow region but, as the hopper inclination increases (β decreases) arches cannot develop anymore and a crossover to a mass flow regime arises. The flow of the particles in this scenario can be considered as radial and the mathematical treatment of the problem changes.

Following the liminar ideas of Brown and Richards [27], and Carleton [28], we analyze the flow of the particles by making a balance of the forces acting on them at an inclined outlet.

Assuming that particles flow radially, they are accelerated from v to $\mathrm{v} + \mathrm{dv}$ as they move from the distance R to $R - dR$ from the vertex O. Figure 6 sketches the situation. Thus, writing the continuity equation for the present geometry we find:

$$\frac{d\mathrm{v}_R}{dR} = \frac{\mathrm{v}_R}{R} \tag{5}$$

and the radial acceleration becomes:

$$a = \mathrm{v}_R \frac{d\mathrm{v}_R}{dR} = \frac{\mathrm{v}_R^2}{R} \tag{6}$$

When evaluating the force on an element of mass *m* we find:

$$ma = m\frac{\mathrm{v}_R^2}{R} \tag{7}$$

Considering that the bulk density does not change appreciably all along radial and continuous flow trajectories, we can apply Eq. (7) throughout the wedged outlet down to the orifice. The gravitational force component applied on the particles belonging to a stream tube at an angle θ respect to the vertical is proportional to $gcos\theta$ and if we write down the force balance for a mass *m* at the outlet orifice it results:

$$m\frac{v_o^2}{R_o} = mgcos\theta \tag{8}$$

The value of R_o is related with the size of the orifice and with the inclination β of the hopper lateral walls, through:

$$R_o = \frac{D}{2sin\beta} \tag{9}$$

Thus, combining the last equations, we get the expression for the velocity at the outlet orifice as a function of the angle of the stream tube and the geometry of the hopper:

$$v_o = \left(\frac{gDcos\theta}{2sin\beta}\right)^{1/2} \tag{10}$$

The mass flow rate can be calculated through the integration of the velocity field at the outlet area, where we have to account for the empty annulus correction at the lateral edges. The vertical component of the velocity contributing to the flow is $v_0 cos\theta$, and the integral to be solved thus becomes:

$$W = \rho\, 2\, L \int_0^{(D-d_p)/2} \left(\frac{gDcos\theta}{2sin\beta}\right)^{1/2} cos\theta\, dx \tag{11}$$

We have to note the dependence of $cos\theta$ on x through the relation: $cos\theta = \frac{\left({R_0}^2 - x^2\right)^{1/2}}{R_0}$.

In this way, the final expression to be integrated is:

$$W = \rho \left(\frac{2g}{sin\beta}\right)^{1/2} L \left(D - d_p\right)^{1/2} \int_0^{(D-d_p)/2} \left[1 - \left(\frac{x}{R_0}\right)^2\right]^{3/4} dx \tag{12}$$

where we introduce the correction of the empty annulus as before.

The integral in Eq. (12) has a numerical solution that allows calculating, almost exactly, the desired flow as soon as the radial flow assumption be valid and $\beta \leq \theta_{app}$. Note the advantage that none parameter is needed in the expression, however the equation goes to infinity when β approaches to zero.

Eq. (4) along with Eq. (12) conform one possible model description of all the flow regimes where the only parameter involved is δ. Nevertheless, to amend the non finite value for β = 0, we can introduce the fluid drag force in Eq. (8) under certain assumptions like spherical shape for the particles, non interacting particles and flow parameters unchanged by particle acceleration or velocity [28]. The introduction of this term makes hard to calculate the integral in Eq. (12). Thus, we make an approximation considering that β is small, and thus $cos\ \theta$ is roughly equal to 1 in Eq. (10), avoiding the subsequent integral calculus. This gives rise to the following expression for the velocity at the outlet:

$$v_o = \left(\frac{gD}{2sin\beta + \frac{C_d \rho_{air}}{m_p} DA} \right)^{1/2} \quad (13)$$

where $A = \pi \frac{{d_p}^2}{4}$ is the cross section area of the particle, ρ_{air} is the air density, m_p is the mass of the particle and C_d is the fluid drag coefficient. The mass flow rate then becomes:

$$W = \rho L \left(D - d_p\right) v_o \quad (14)$$

We will show that Eq. (14) can be used as a good approximation for all the range of angle β. Although C_d could be determined experimentally, we don't know its value for the different seeds employed in this work and, for that reason, we keep it as a free parameter.

Moreover, it is worthy to note that the dependency of the form $(\sin\beta)^{-1/2}$ has already been proposed in the past [35]. As pointed in the introduction, authors in that work discuss in an appropriated way the mass discharge rate of conical hoppers using an elastoplastic model implemented with an Eulerian finite element method approach. Like we will see below in our present model, they conclude that a continuum-like derivation of the mass discharge rate represents in a good way both experimental and DEM results. Nevertheless, the collective behavior of many particles interacting with each other is still a challenge and has to be taken into account in detail.

In the next section we present experimental results for the discharge of a wedged silo and compare the capability of Eqs. (4), (12) and (14) to predict the whole range of flows expected when the angle of the hopper varies from 90º to 0º.

4. Experimental results and theoretical predictions

In this section we present the results obtained for a sequence of discharges using the three different seeds described in Section 2.

We perform over ten equal realizations for each type of seed and each value of the outlet angle, β, keeping fixed the outlet diameter D. Ambient humidity is measured before each experiment and the working range values are from 22% to 36%, thus avoiding the presence of capillary effects in the discharges.

Figure 7 shows the flow rate of seeds as a function of the hopper angle. The three parts of the figure correspond to millet, sesame and canary seeds, respectively. The experimental results are represented by filled circles, while the theoretical predictions of Eq. (12) are given by the solid line when $\beta \leq \theta_{app}$, *i.e.*, mass flow regime. The horizontal line represents the value given by Eq. (4) and is valid when $\beta \geq \theta_{app}$., *i.e.*, for funnel flow. The intersection of the two curves is referred as the angle of approach for each particle system in the figure. The values indicated for θ_{app} correspond to those determined, as an average, by direct observation on a video of the discharge during the experiments, they are accompanied by a bar representing their dispersion. The values for the expected constant flow in the funnel regime are indicated in each part. They are calculated using Eq. (4) with D =11mm and the value of δ coming from the fitting results in Figure 5.

For the three seeds, the agreement between experiments and theory is quite good, considering that just one parameter is used for funnel flow and none is needed for mass flow. Indeed, the horizontal line represents the constant flow obtained from Eq. (4),

where the value of δ used is the one resulting from the fits of the data in each case (Figure 5). On the other hand, the theoretical prediction from Eq. (12) involves known parameters that are determined through direct measurement of the bulk density and the geometry of the particles and the silo.

Finally, we show in the same figure the results coming from the application of Eq. (14), represented by the empty squares and the dashed line. For the calculations we use $\rho_{air} = 1.22\ kg/m^3$ and the respective mass and cross area of the seeds. Given that the exact value of the drag constant, C_d, for each seed is unknown, we estimate it by choosing the value which better fits the experimental data. The obtained values are: 5, 5 and 7 for sesame, canary seed and millet, respectively. These values are in the expected range considering that the Reynolds numbers involved in the problem are less than 200, i.e., in the so called intermediate zone [28, 37].

Finally, it is important to note that the role of the drag term is relevant only near $\beta = 0$, while for $\beta > 0$ the sine term dominates. Because our particles are not too heavy, a difference is observed in the results obtained through the different equations, but, were the particles heavier (like for instance the case of glass beads), the differences would not be appreciable.

5. Discussion

From the experiments shown so far we are able to distinguish the two main regimes found in a silo discharge as the angle of inclination of the hopper changes. For steep walls (small β), the mass flow regime is characterized by a radial velocity dynamic and

its theoretical description can be simply followed by a radial continuum flow picture. Although the equation relating the dependence of W on the silo and grains has not an exact solution but a numerical one, no parameters are needed to understand the basic physics behind the problem, at least for the particular geometry used in the present experiments. The equation resulting from this approach describes quite well all the results.

As β increases, the radial dynamics changes because of the presence of stagnant zones of particles moving more slowly over the walls of the hopper. The radial description is no more valid and has to be changed; the concept of a granular flow has to be introduced and the funnel flow regime begins. Indeed, the stagnant zones favor the formation of arches of particles that find the way of stabilize, at least for a short time, force chains between the grains, slowing down the flow at the outlet. The formation and breaking of these arches is the clue to understand the fluctuations often observed in the discharge of grains. As soon as an arch is stable at the outlet (standing as a vault supported by the particles in the stagnant zone) the particles above it stack for a moment and, when the arch destabilizes, they initiate a free fall with almost zero initial velocity. Assuming a parabolic shape for the vault, an expression for the flow rate can be calculated with the sole inclusion of one parameter related to the shape of the parabolic vault, i.e., δ. In this way, as $\beta \geq \theta_{app}$, the dynamic of formation and destruction of the arches dominates the funnel flow regime and the flow rate becomes independent of β. By performing a set of experiments with different outlet apertures, D, the parameter δ can be calculated through a data fitting (Figure 5). The values obtained for δ are in agreement with the results of Börzsönyi *et al.* [36] in the sense that the shape of the dome formed at the outlet of the silo, where the density of particles is lower, has a height that decreases for more elongated particles. This reinforces the meaning to the

parameter introduced by Oldal *et al.* [25], making Eq. (4) to be a simple and practical way to describe the results and any others deduced for other geometries.

It is important to note that theoretical results are expected to be very sensitive to the selected value for d_p, especially for seeds being far apart from a spherical shape or with a wide size distribution. This feature makes δ to change depending on the selected value of d_p used to represent the particles. Besides, it is expected that the scale of the vault will not likely to be conserved as D changes. For that reason, and in order to determine δ, we choose to make a fit on a complete set of data for different values of D and we always take d_p as given by Eq. (1).

Thus, all the range of flows can be described with this dual dynamic, where the intersection of the two curves describing each regime gives the internal angle of approach, θ_{app}, as can be appreciated in Figure 7. The values of this angle can be verified in our experiments through direct observation from a video of the discharge.

The theoretical prediction of Eq. (14) is almost as good as the one obtained from the former equations (separating the flow into two regimes) and it has the advantage of describing quite well the behavior for all the range of inclination angles in just one equation. Its predictions are less accurate for the case of canary seed, where it is evident that the flow is overestimated for the larger angles. This is related to the assumption that a radial velocity picture can be applied to all the range of hopper inclinations which, for the case of elongated particles, is more difficult to sustain. Indeed, as can be appreciated in the dynamic of the discharge, the nematic of the particles is such that, close to the aperture, the orientation of them at the stagnant or quasi stagnant zones is parallel to the orientation of the hopper, making them more stable and, thus, more difficult to move. For β close to 90º, particle orientation is practically perpendicular to that of the particles in streams closer to the vertical [36]. The overestimation of the flow could also be

referred to as an effect due to the particular value taken in Eq. (14) for d_p, because if this value were taken as closer to the real "empty annulus" effect, it should well be considered to be greater than that resulting from Eq. (1).

Conclusions

We performed experiments with different seeds discharging from a silo with a wedged outlet geometry to study the dependence of the flow rate on the inclination angles, β, from 0º to 90º, i.e., examining the flow patterns from mass to funnel flow.

We show that a theoretical model can be used to predict the behavior in the funnel flow region using only one parameter, δ, with a simple geometrical interpretation, in agreement with the findings of other authors [25] while, for the case of mass flow, the assumption of a radial velocity in the flow streams is enough to describe quite well the results. These two different dynamic predictions meet in the proximity of the internal angle of approach of the grains, θ_{app}, where the transition of the regime is expected. In this way, the crossing of the descriptions given by Eq. (4) and (12) helps to determine the transition zone angle, otherwise difficult to measure.

Parameter δ is directly related to the shape of the vault formed at the outlet of the silo in the funnel regime. Nevertheless, the fact that its experimental determination is quite difficult, makes it to still preserve the fitting character. This parameter shows an increasing trend when the form factor of the particles decreases and we may expect that, under very well controlled conditions, δ could have some generality for a particular group of materials.

It is expected that appropriate changes can be introduced from Eq. (2) to Eq. (12) to account for any other type of hopper and/or silo geometry. In the same way, wider size

distributions for particles will necessary affect the results and should be brought into the theoretical calculations.

Through Eq. (14) we also introduce a model based on the hypothesis that radial velocity behavior is valid inside all the range of values for β. This assumption allows introducing a drag force term in the equations and the resolution of the final expression for the flow velocity can be attained very easily with the sole presence of one parameter related to the drag coefficient of the grains due to the presence of air flow. While this last modeling has the advantage of predicting the whole behavior using just one equation, even valid for $\beta = 0^{o}$, it overestimates the flow rate for elongated particles. Besides, the continuum approaches of equations like Eq. (12) and Eq. (14) still have the drawback of neglecting the particle properties. We prove they give an overall good prediction but they still cannot account for the difference among different particles.

Future application of the present theoretical description to other silo geometry and other type of particles is necessary to prove which one is the most realistic in each case and to add the contribution of the form factors of the particles (like, for instance FF) to parameters like δ.

Acknowledgements

Authors want to acknowledge financial support from Universidad Nacional de San Luis through PROICO 310114 and from CONICET through PIP 353. Especial thanks are due to the professional support of Engineer V. Schmidt in the design and construction of the experimental set up.

References

[1] F. Pacheco-Vázquez, A.Y. Ramos-Reyes, S. Hidalgo-Caballero, Surface depression with double-angle geometry during the discharge of grains from a silo, Physical Review E 96 (2017) 022901.

[2] R.O. Uñac, O.A. Benegas, A.M. Vidales and I. Ippolito, Experimental study of discharge rate fluctuations in a silo with different hopper geometries, Powder Technology 225 (2012) 214–220.

[3] R.T. Fowler, J.R. Glastonbury, The flow of granular solids through orifices, Chemical Engineering Science 10 (1959) 150–156.

[4] W.A. Beverloo, H.A. Leniger, J. van de Velde, The flow of granular solids through orifices, Chemical Engineering Science 15 (1961) 260–269.

[5] K. Grudzien, Analysis of the granular material concentration changes during silo discharging process based on x-ray image analysis, Image Processing & Communication 19 (2015) 107–118.

[6] L. Babout, K. Grudzien, E. Maire, P.J. Withers, Influence of wall roughness and packing density on stagnant zone formation during funnel flow discharge from a silo: An X-ray imaging study, Chemical Engineering Science 97 (2013) 210–224.

[7] J.F. Wambaugh, Simple models for granular force networks, Physica D 239 (2010) 1818–1826.

[8] S. Albaraki, S.J. Antony, How does internal angle of hoppers affect granular flow? Experimental studies using digital particle image velocimetry, Powder Technology 268 (2014) 253–260.

[9] A. Anand, J.S. Curtis, C.R.Wassgren, B.C. Hancock, W.R. Ketterhagen, Predicting discharge dynamics from a rectangular hopper using the discrete element method (DEM), Chemical Engineering Science 63 (2008) 5821–5830.

[10] C. Gonzáles-Montellano, F. Ayuga, J.Y. Ooi, Discrete element modelling of grain flow in a planar silo: influence of simulation parameters, Granular Matter 13 (2011) 149–158.

[11] J. Wu, J. Binbo, J. Chen, Y. Yang, Multi-scale study of particle flow in silos, Advanced Powder Technology 20 (2009) 62–73.

[12] R. Balevičius, R. Kačianauskas, Z. Mróz, I. Sielamowicz, Discrete-particle investigation of friction effect in filling and unsteady/steady discharge in three-dimensional wedge-shaped hopper, Powder Technology 187 (2008) 159–174.

[13] C.A. Calderón, M.C. Villagrán Olivares, R.O. Uñac, A. M. Vidales, Correlations between flow rate parameters and the shape of the grains in a silo discharge, , Powder Technology 320 (2017) 43–50.

[14] S. Humby, U. Tüzün, A.B. Yu, Prediction of hopper discharge rates of binary granular mixtures, Chemical Engineering Science 53 (1998) 483–494.

[15] S.D. Liu, Z.Y. Zhou, R.P. Zou, D. Pinson, A.B. Yu, Flow characteristics and discharge rate of ellipsoidal particles in a flat bottom hopper, Powder Technology 253 (2014) 70–79.

[16] A.W. Jenike, J.R. Johansson, J.W. Carson, Bin loads – part 2: Concepts ASME, Journal of Engineering for Industry 95 (1973) 1–5.

[17] DIN 1055 Teil 6, Lastannahmen für Bauten, Lasten in Silozellen, 1987.

[18] EUROCODE 1 PART 4. Actions on silos and tanks. Bruxelas, 1995.

[19] AS 3774 – Loads on bulk solids containers – 1996.

[20] International Standard ISO 11697 Technical Committee ISO/TC 98, Bases for design of structures, Subcommittee SC 3, Loads, forces and other actions.

[21] A. Drescher, On the criteria for mass flow in hoppers, Powder Technology, 73 (1992) 251–260.

[22] D. M. Walker, An approximate theory for pressures and arching in hoppers, Chemical Engineering Science 21 (1966) 975–997.

[23] A.W. Jenike, New developments in the theory of particulate solids flow, EFCE, Serie Nº49, Bergen, Norway.

[24] A.W. Jenike, A theory of flow of particulate solids in converging and diverging channels based on a conical yield function, Powder Technology 50 (1987) 229–236.

[25] I. Oldal, I. Keppler, B. Csizmadia, L. Fenyvesi, Outflow properties of silos: The effect of arching, Advanced Powder Technology 23 (2012) 290–297.

[26] J. Mellmann, T. Hoffmann, C. Fürll, Mass flow during unloading of agricultural bulk materials from silos depending on particle form, flow properties and geometry of the discharge opening, Powder Technology 253 (2014) 46–52

[27] R.L. Brown and J.C. Richards, Principles of Powder Mechanics, Pergamon Press, 1st Edition (1770).

[28] A.J. Carleton, The effect of fluid-drag forces on the discharge of free-falling solids from hoppers, Powder Technology 6 (1972) 91–96.

[29] H.E. Rose, T. Tanaka, Rate of discharge of granular materials from bins and hoppers, Engineer 208 (1959) 465–469.

[30] R.M. Nedderman, U. Tüzün, The flow of granular materials –I. Discharge rates from hoppers, Chemical Engineering Science 37 (1982) 1597–1609.

[31] F. Vivanco, S. Rica, F. Melo, Dynamical arching in a two dimensional granular flow, Granular Matter 14 (2012) 563–576.

[32] G. Mollon, J. Zhao, Characterization of fluctuations in granular hopper flow, Granular Matter 15 (2013) 827–840.

[33] J. Duran, Sands, Powders, and Grains. An Introduction to the Physics of Granular Materials, Springer Science, 2000.

[34] L. Staron, P. -Y. Lagrée, S. Popinet, Continuum simulation of the discharge of the granular silo, The European Physical Journal E 37 (2014) 5.

[35] Q.J. Zheng, B.S. Xia, R.H. Pan, A.B. Yu, Prediction of mass discharge rate in conical hoppers using elastoplastic model, Powder Technology 307 (2017) 63-72, and references therein.

[36] T. Börzsönyi, E. Somfai, B. Szabó, S. Wegner, P. Mier, G. Rose, R. Stannarius, Packing, alignment and flow of shape-anisotropic grains in a 3D silo experiment, New Journal of Physics 18 (2016) 093017.

[37] N-S. Cheng, Comparison of formulas for drag coefficient and settling velocity of spherical particles, Powder Technology 189 (2009) 395–398.

Figure Captions

Figure 1: Schematic representation of the set up used in the experiments. The plot shows a typical discharge where the mass vs. time is recorded to calculate, from the linear fit indicated by the line, the slope corresponding to the flow rate.

Figure 2: Photographs of the three types of seeds used in the experiments: (a) millet, (b) sesame and (c) canary seed. They are shown over a graph paper of 1 millimeter scale.

Figure 3: A close-up photo of a mass discharge of millet in a flat-bottomed silo. The angle θ_{app} is indicated (approximately 30º for those seeds). Three zones are distinguished according to the velocity of the grains: the central part with a high flow; the intermediate one with a slow movement and the stagnant zone, typical in the $\beta = 90^{o}$ case. Note that the grain close to the aperture is screening the orifice ("empty annulus" effect [27, 28]).

Figure 4: Sketch of the geometry of the arch temporarily formed at the outlet of the hopper. Particles are assumed to freely fall from this arch of shape *f(x,y)*. At the right, a front draw of the parabolic surface is shown to indicate the height *h*. Parameter δ is calculated as the ratio of *h* and the corrected outlet aperture $D - d_p$.

Figure 5: Experimental results for silo discharge with different apertures *D*. The line corresponds to the fit performed using Eq. (4) with δ as the only parameter. As indicated in each part, the data correspond to: (a) millet, (b) sesame and (c) canary seed.

Figure 6: Sketch of the trajectory of a particle at position R from the vertex of the wedged hopper, flowing radially with a velocity v in a flow stream subtending an angle θ with the vertical.

Figure 7: Experimental results (filled circles) for the discharge of the silo with constant aperture of 11 mm and variable angle β for (a) millet, (b) sesame and (c) canary seed. The comparison with the two theoretical models developed in the text is presented. The bar indicates de zone close to the value of the angle of approach where the transition from mass flow to funnel flow is expected.

Table 1: Values for different parameters of the seeds used in experiments

	Millet	Sesame	Canary seed
length (mm)	3.4 ± 0.2	3.4 ± 0.2	6.0 ± 0.3
width (mm)	2.3 ± 0.2	2.1 ± 0.2	2.2 ± 0.2
FF	1.5 ± 0.4	1.6 ± 0.3	2.8 ± 0.4
d_p (mm)	2.7 ± 0.2	2.5 ± 0.1	3.1 ± 0.2
ρ_b (kg/m^3)	780 ± 10	640 ± 10	760 ± 10
δ	0.86 ±0.02	0.65 ±0.01	0.41 ±0.01

- Model silo discharge experiments in a wedged hopper geometry for all range of angles
- Two possible theoretical descriptions are developed with just one parameter
- First model can estimate the internal angle of approach of the particles
- Second model predicts mass and funnel flow rates using a single equation

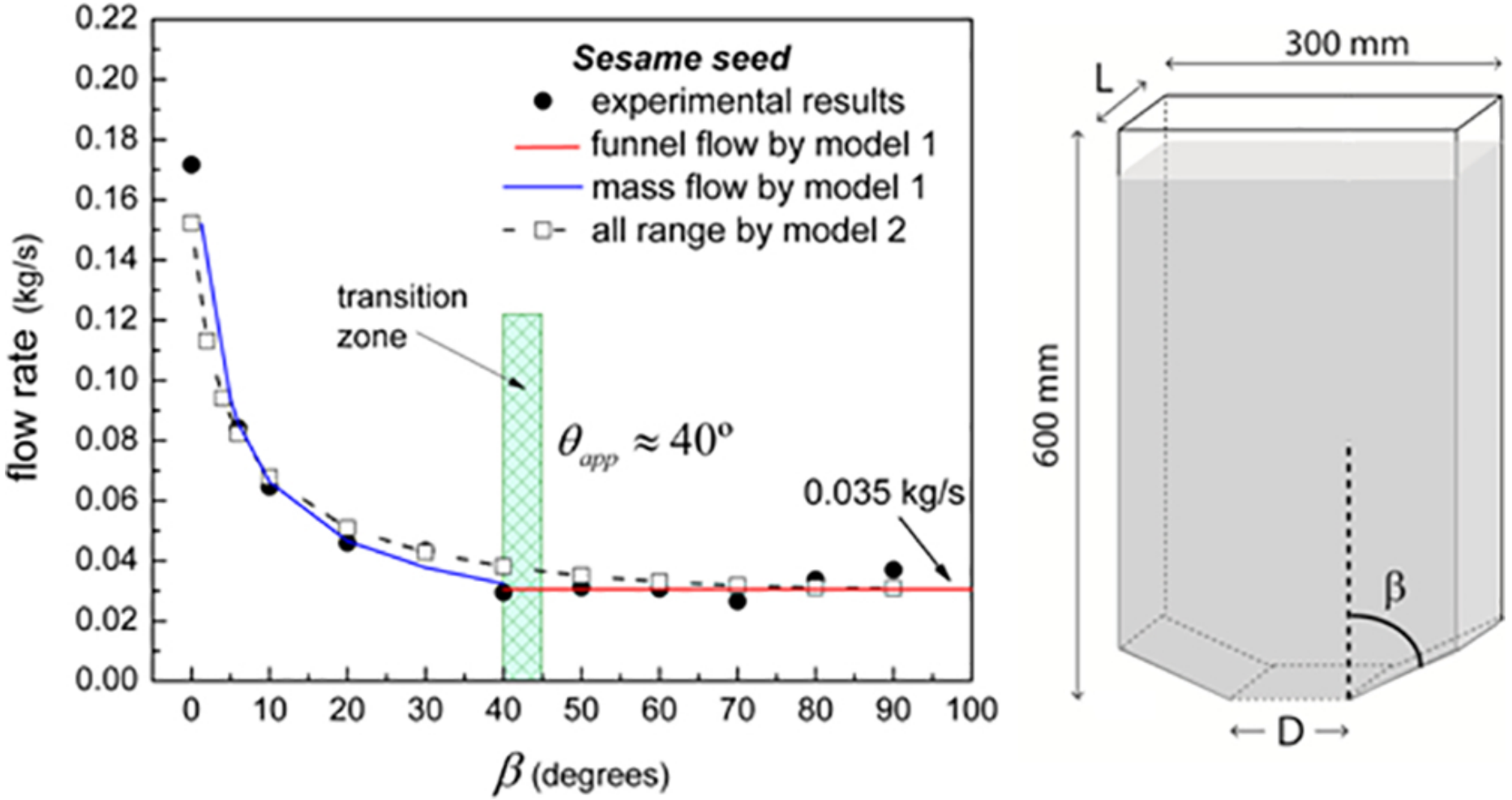

Graphics Abstract

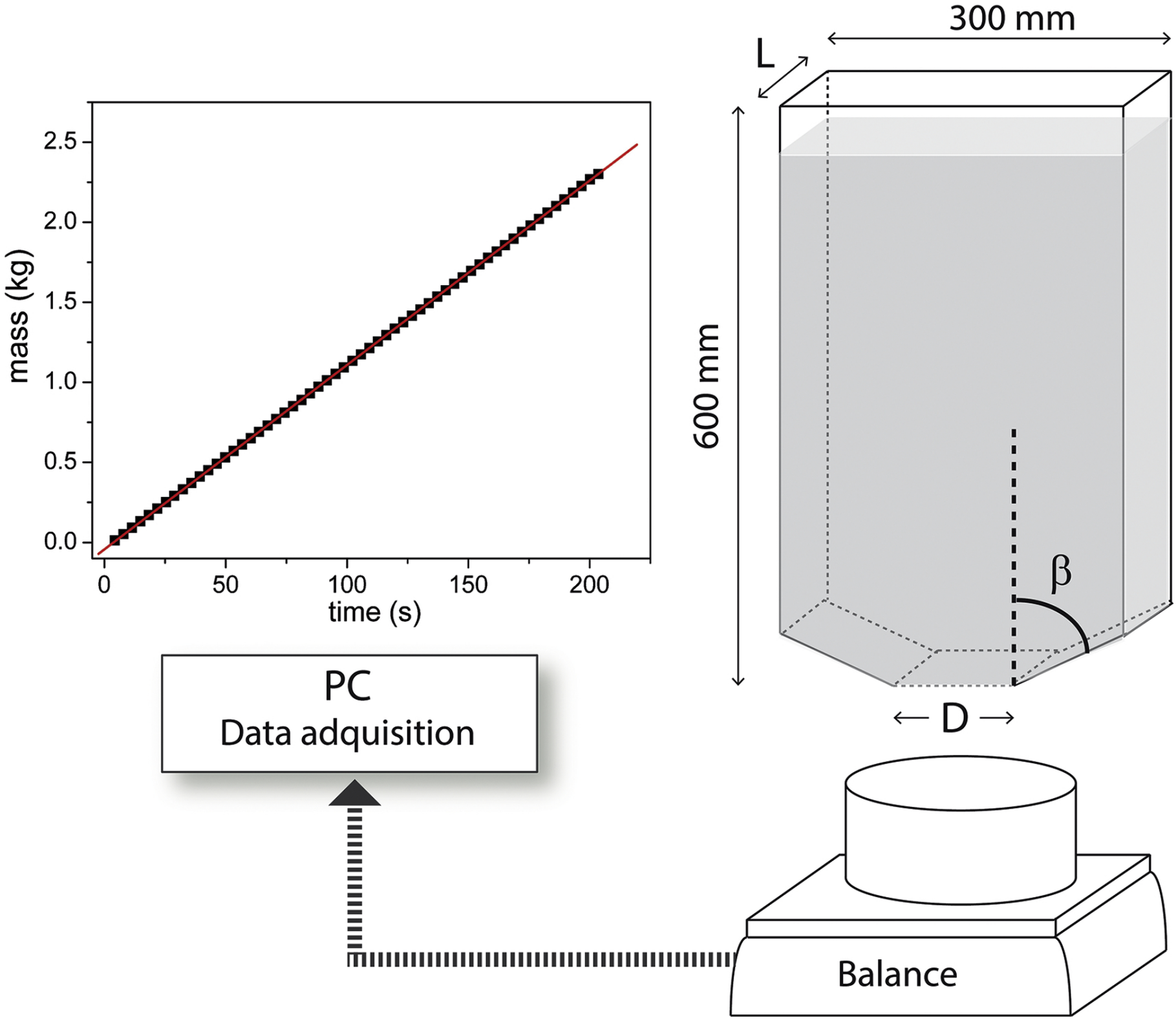
300 mm
L
600 mm
β
D
mass (kg)
time (s)
0.0
0.5
1.0
1.5
2.0
2.5
0
50
100
150
200
PC
Data adquisition
Balance

Figure 1

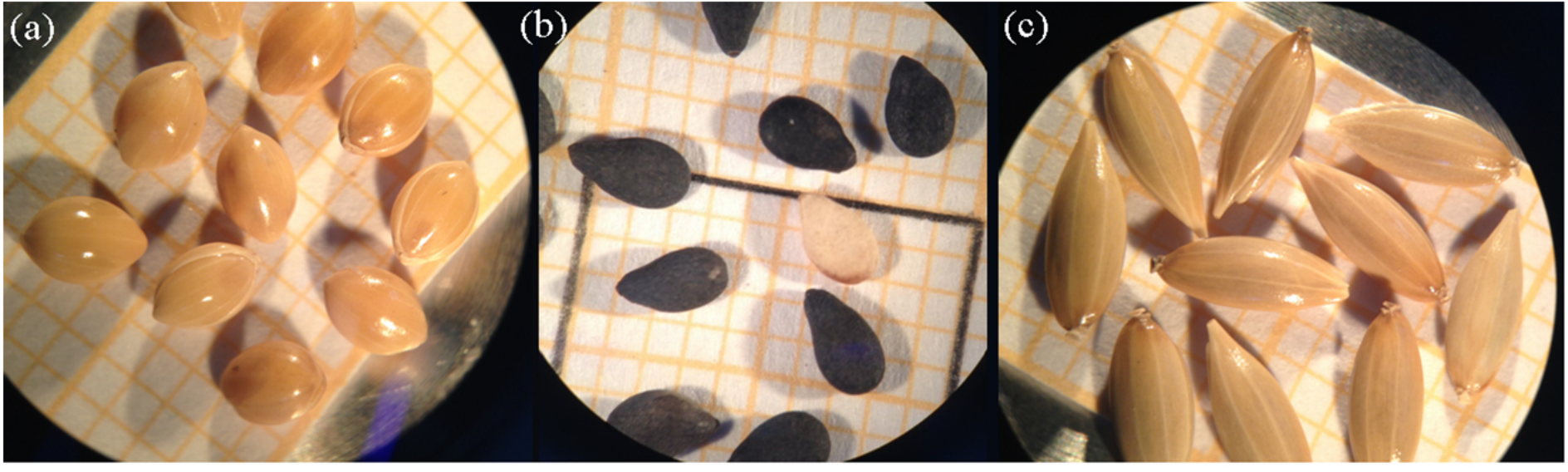

Figure 2

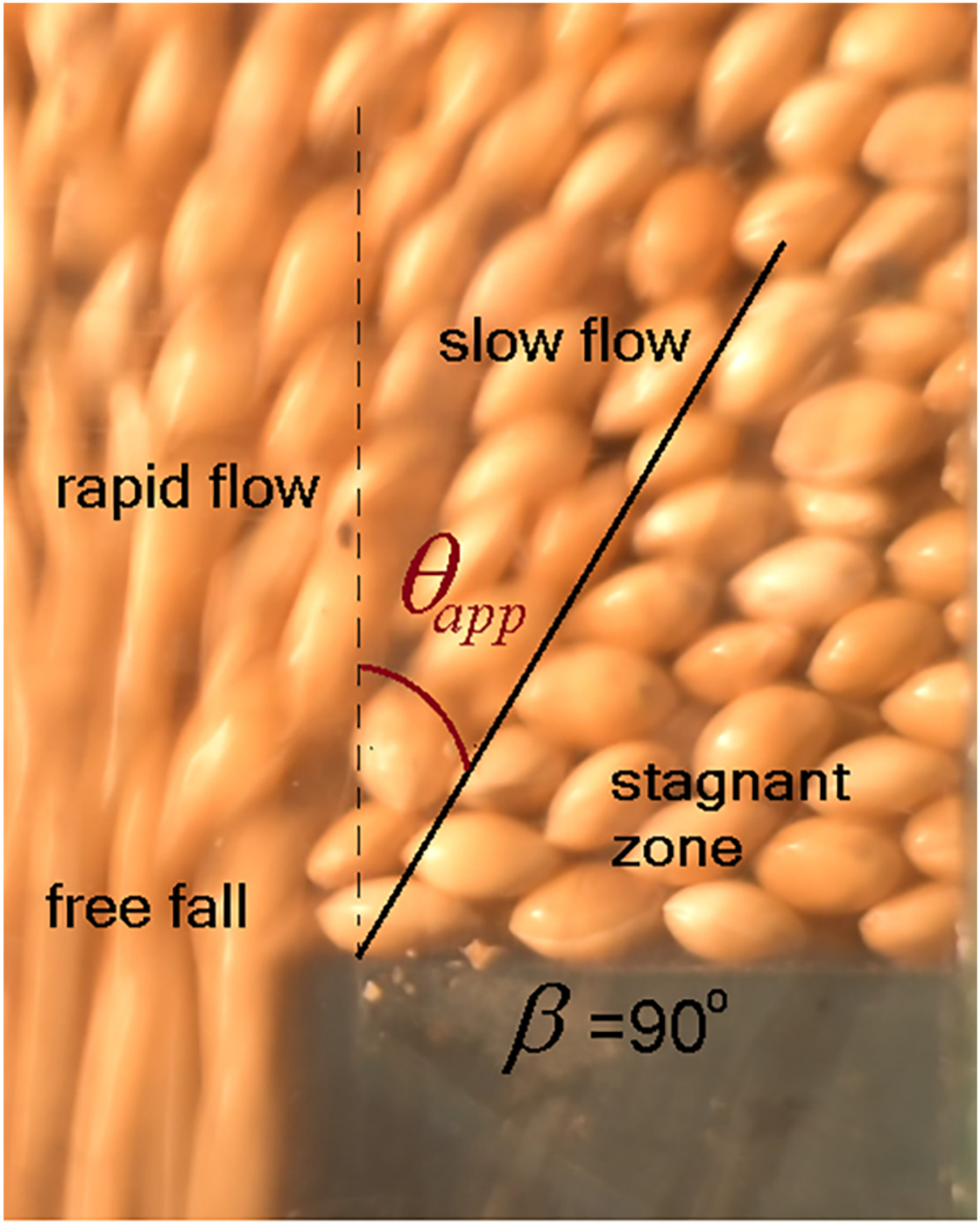
slow flow
rapid flow
θ_{app}
stagnant
zone
free fall
β =90°

Figure 3

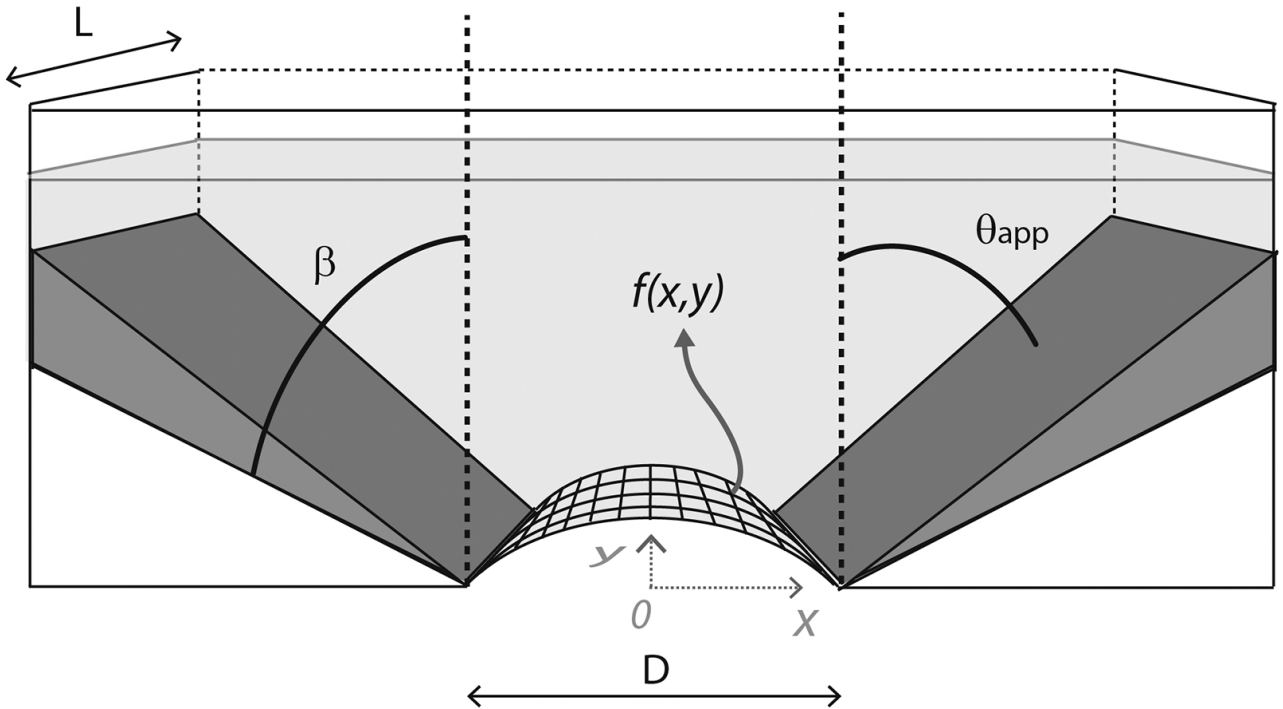

$$f(x,y) = h\left(1 - \left(\frac{2x}{D - d_p}\right)^2\right)$$

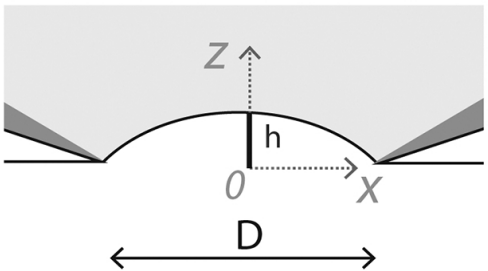

$$\delta = h/(D - d_p)$$

Figure 4

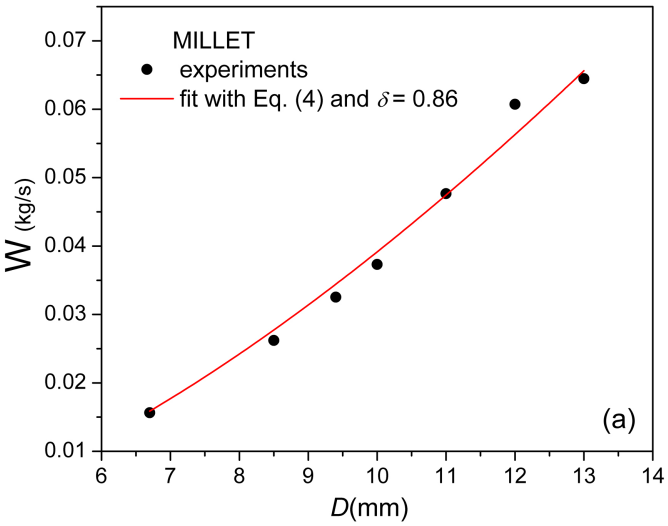
MILLET
experiments
fit with Eq. (4) and δ = 0.86
W (kg/s)
D(mm)
(a)

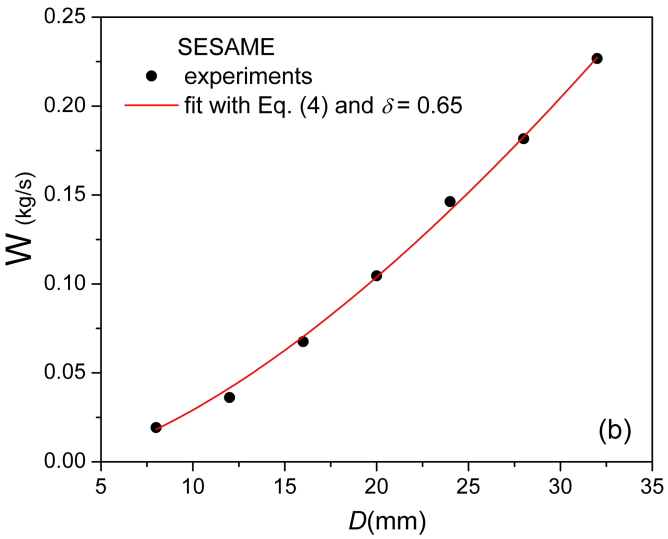
SESAME
experiments
fit with Eq. (4) and δ = 0.65
W (kg/s)
D(mm)
(b)

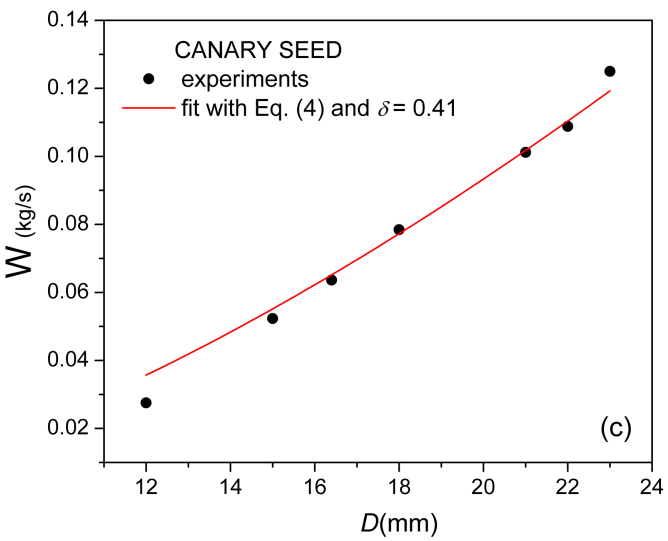
CANARY SEED
experiments
fit with Eq. (4) and δ = 0.41
W (kg/s)
D(mm)
(c)

Figure 5

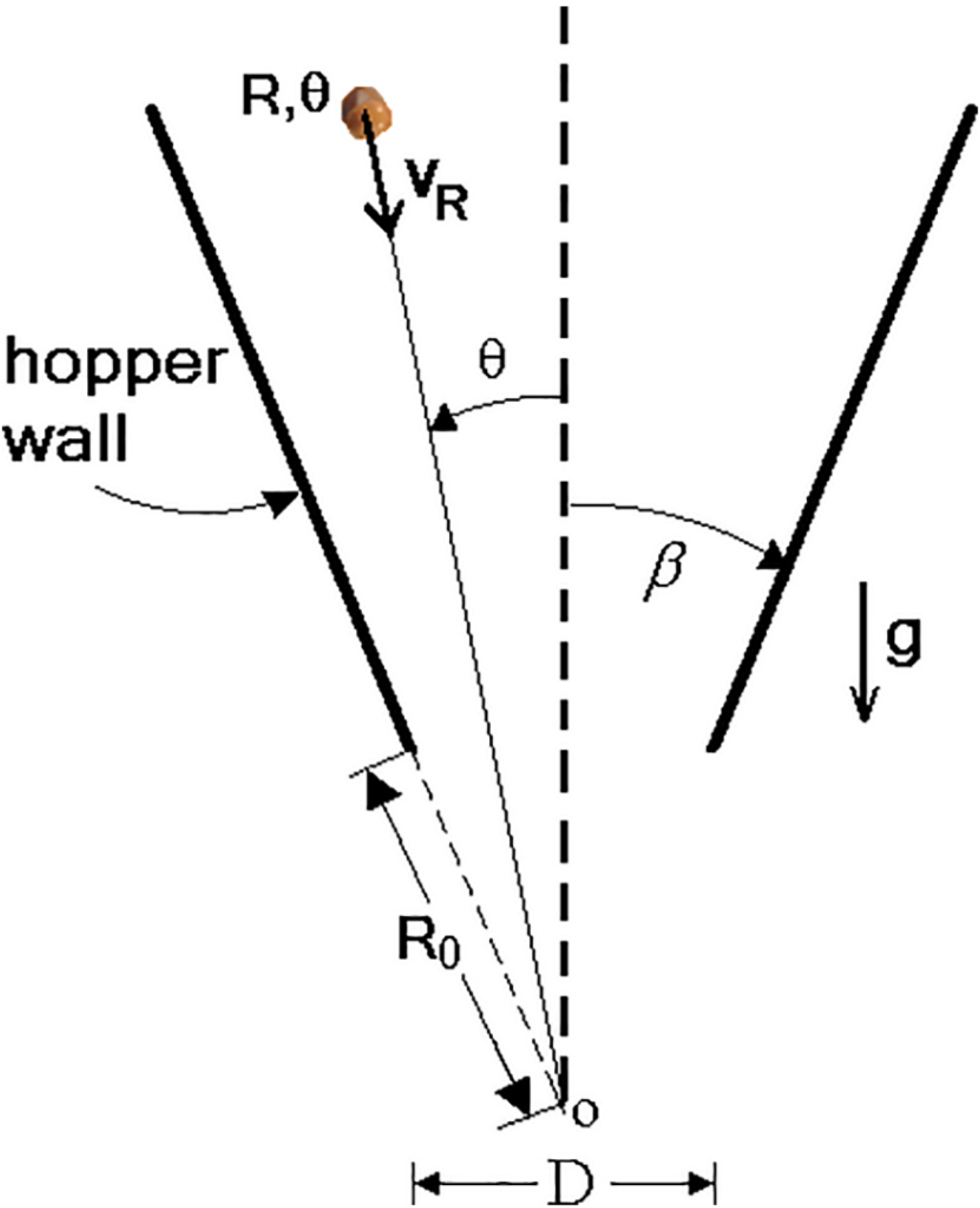

Figure 6

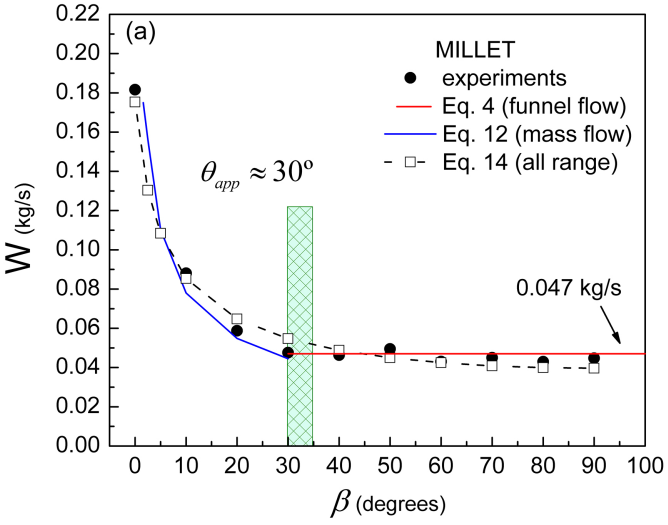
(a)
MILLET
experiments
Eq. 4 (funnel flow)
Eq. 12 (mass flow)
Eq. 14 (all range)
$\theta_{app} \approx 30^o$
0.047 kg/s
W (kg/s)
β (degrees)

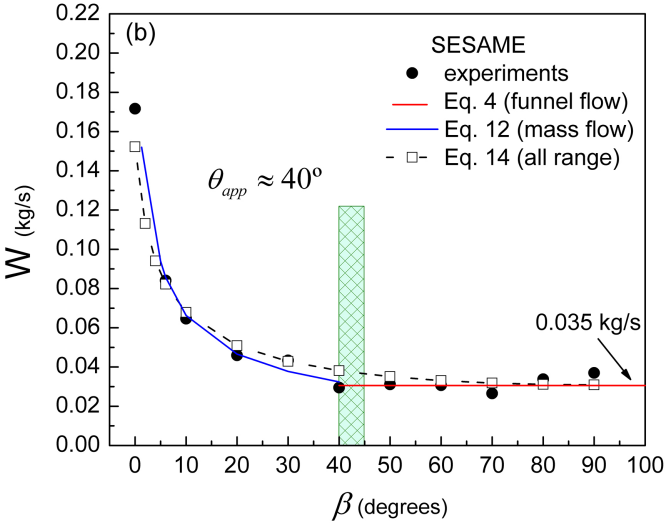
(b)
SESAME
experiments
Eq. 4 (funnel flow)
Eq. 12 (mass flow)
Eq. 14 (all range)
$\theta_{app} \approx 40^o$
0.035 kg/s
W (kg/s)
β (degrees)

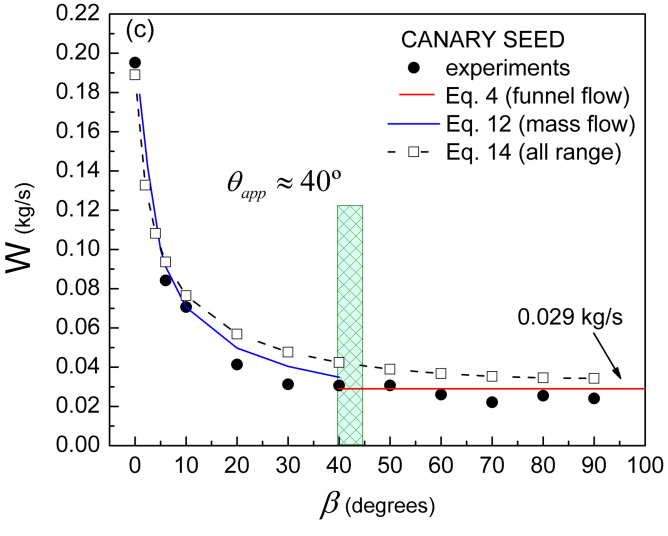
(c)
CANARY SEED
experiments
Eq. 4 (funnel flow)
Eq. 12 (mass flow)
Eq. 14 (all range)
$\theta_{app} \approx 40^o$
0.029 kg/s
W (kg/s)
β (degrees)

Figure 7